metals

MDPI

Article

Influence of Temperature on Mechanical Properties of AMCs

E.S. Caballero [1,*], Fátima Ternero [1], Petr Urban [1], Francisco G. Cuevas [2] and Jesús Cintas [1]

[1] Escuela Técnica Superior de Ingeniería, Universidad de Sevilla, Camino de los Descubrimientos s/n, 41092 Sevilla, Spain; fternero@us.es (F.T.); purban@us.es (P.U.); jcintas@us.es (J.C.)

[2] Escuela Técnica Superior de Ingeniería, Universidad de huelva, Campus La Rábida, Carretera Palos s/n, 21819 Palos de la Frontera, Spain; fgcuevas@dqcm.uhu.es

* Correspondence: esanchez3@us.es; Tel.: +34-954-487-313

Received: 27 May 2020; Accepted: 10 June 2020; Published: 12 June 2020

Abstract: This research focused on studying the effect of temperature on the mechanical properties of aluminium matrix composites (AMCs) obtained by a powder metallurgy route. Aluminium powder was milled at room temperature for 5 h and using different atmospheres in order to achieve different amounts of reinforcement. The atmospheres employed were vacuum, confined ammonia, and vacuum combined with a short-time (5 and 10 min) of ammonia gas flow. After mechanical alloying, powders were consolidated by cold uniaxial pressing (850 MPa) and vacuum sintering (650 °C, 1 h). hardness and tensile tests, on consolidated samples, were carried out at room temperature. Subsequently, the effect of temperature on both properties were evaluated. On one hand, the UTS and hardness were measured, again at room temperature, but after having subjected the sintered samples to a prolonged annealing (400 °C, 100 h). On the other hand, the tensile and hardness behaviour were also studied, while the samples are at high temperature, in particular 250 °C for UTS, and in the range between 100 and 400 °C for hardness. Results show that the use of ammonia gas allows achieving mechanical properties, at room and high temperature, higher than those of the commercial alloys EN AW 2024 T4, and EN AW 7075 T6.

Keywords: AMCs; mechanical alloying; mechanical properties; temperature

1. Introduction

Nowadays, lightweight (low-density) alloys are extraordinarily attractive for industries such as transport, because they make it possible to reduce weight, which will ultimately translate into a reduction in fuel consumption and polluting effects [1,2].

Therefore, in the automotive and aeronautics industries, aluminium and its alloys play an important role in a wide range of structural applications [3–5]. Unfortunately, there is a limiting factor for their use: the mechanical properties of aluminium alloys can be degraded when the material is exposed to temperatures above 100 °C (373 K). Consequently, it is of great interest to improve the properties of aluminium, both at room and at high temperatures, mainly in terms of reducing properties degradation.

One of the possible ways to improve the properties of aluminium alloys is to reinforce them with ceramic particles, thus obtaining aluminium matrix composite materials (AMCs). These AMCs have interesting properties for industry, such as excellent wear resistance, higher specific resistance and higher resistance to thermal degradation, compared to conventional aluminium alloys [6,7]. Other properties of AMCs are their improved corrosion resistance, good thermal and electrical conductivity, and high

damping capacity [8]. For all these reasons, AMCs have aroused great interest in the academic and industrial sectors, especially in the transport and aerospace industries [9].

AMCs are already used in the manufacture of aerospace and automotive components, such as gear parts, crankshafts, suspension arms, ventral fins, fuel access door covers, and rotating blade sleeves, among others. In the electronics industry, they are used to manufacture integrated heat sinks, microwave housings, and microprocessor lids. Most of these applications involve operation under varying temperature conditions [10]. In addition, structural components used in the aerospace industry, such as fuselage frames, aircraft wings, and landing gears are usually exposed to severe thermal gradients created by aerodynamic heating [11,12]. Therefore, it is advisable to study the effect of temperature on the properties of the material, because high temperatures can cause chemical reactions between the reinforcements and the matrix, which results affecting the bonding forces between them, and the integrity of the material.

Moreover, the ceramic phases generally used as a reinforcement in AMCs have very different coefficients of thermal expansion (CTE) to that of the aluminium. This mismatch can cause large residual thermal stresses near the matrix–reinforcement interfaces, which were initiated in the cooling stage during the manufacturing process [13,14]. These residual stresses usually reduce the mechanical and physical properties of the composite material, and they often cause its premature failure [15]. There are several mechanisms whereby thermal stresses can be relaxed, including interface detachment, microplasticity of the metal matrix, and crack initiation and propagation [16]. AMCs are frequently exposed to cyclic thermal temperature conditions, which are often especially critical, and accelerate material degradation [13].

Some recent studies are aimed at determining which types of reinforcements produce the best mechanical properties and which of them mitigate the pernicious effects of temperature [17,18]. Although the use of reinforcements such as alumina (Al_2O_3) and silicon carbide (SiC) has been predominant, alternative reinforcements such as aluminium nitride (AlN), silicon dioxide (SiO_2), boron carbide (B_4C), titanium carbide (TiC), titanium boride (TiB_2), zirconium diboride (ZrB_2), and titanium dioxide (TiO_2) have also been studied. The way in which AMCs are produced has also been analysed. One of the most widespread processes for manufacturing AMCs is powder metallurgy, since it allows obtaining AMCs with good mechanical properties, which in turn is more economical than other types of techniques [19].

The main aim of this work is the detailed study of the mechanical behaviour at the temperature of high-strength AMCs obtained by mechanical alloying of aluminium powder in nitriding atmospheres. The degradation of their mechanical properties, because of high temperature, will be specially treated. There are only a few studies focused on the temperature behaviour of nitride-reinforced metal matrix composites. One of the aims of this work is to contribute to the clarification of this issue in AMCs.

2. Materials and Methods

The starting material consisted of gas atomized elemental aluminium powder (AS 61, Eckart) with a purity level higher than 99.7 wt % and a mean particle size of 80.5 μm (as measured by laser diffraction in a Malvern Mastersizer 2000, Almelo, Netherlands). The aluminium powder was milled in a high-energy attritor ball mill (Union Process, Ohio, USA), having a water cooled stainless steel vessel of 1400 cm^3. Mill charge contained 72 g of powder and 3600 g of balls (charge ratio 50:1). A 3 wt % of ethylene-bis-stereamide (EBS) micropowder organic wax was added as a process control agent (PCA).

All milling experiments lasted 5 h and were performed at room temperature with a rotor speed of 500 rpm. however, three different atmosphere conditions were used: vacuum (5 Pa), confined ammonia gas (1.3×10^5 Pa), and a combination of vacuum (5 Pa) and ammonia gas flow (1 cm^3/s). This last experiment began under vacuum, and after 2 h, a short-time ammonia gas flow was incorporated for a time of 5 or 10 min. Subsequently, milling continued under vacuum until a total time of 5 h was reached. Table 1 summarizes milling conditions for the different experiments.

Table 1. Milling atmosphere conditions.

Milling Experiment	Atmosphere	Sample
I	Vacuum (5 h)	V
II	Confined ammonia gas (5 h)	C
III	Vacuum (2 h) + Ammonia gas flow (5 min) + Vacuum (2 h 55 min)	F5
IV	Vacuum (2 h) + Ammonia gas flow (10 min) + Vacuum (2 h 50 min)	F10

Both cylindrical (diameter: 12 mm; mass: 3 g) and tensile dog-bone-shaped specimens were produced from all milled powders by cold uniaxial pressing (850 MPa) and vacuum (5 Pa) sintering (650 °C for 1 h), followed by furnace cooling. EBS wax was also used as a die-wall lubricant during cold pressing. X-ray diffraction analysis (XRD, Bruker D8 Advance, using CuKα radiation, a step size of 0.015°, and a time step of 0.5 s, Massachusetts, USA) was used to identify and quantify the phases. The XRD studies were carried out on the compacts after their consolidation process, as well as after they were heat treated at 400 °C for 100 h. A universal testing machine (Instron 5505, Massachusetts, USA) with a load cell of 100 kN was used for tensile testing, whereas Vickers hardness (Struers Duramin A300, Willich, Germany) were measured using a load of 1 kg. Fractographic studies were performed using a field emission scanning electron microscopy (FESEM, FEI Teneo, Eindhoven, The Netherlands).

3. Results and Discussion

After milling process, cylindrical and dog-bone-shape specimens were pressed and sintered from the different milled powders, in order to evaluate their hardness (HV) and ultimate tensile strength (UTS), respectively. Both properties were tested under different conditions listed in Table 2. Compacts from as-received aluminium powder were also prepared by comparison purpose.

Table 2. Test conditions.

Heat Treatment after Sintering	Test Temperature	Test	Condition
-	Room Temperature	hardness/Tensile	RT
400 °C, 100 h	Room Temperature	hardness/Tensile	400 °C 100 h/RT
250 °C, 1 h	Room Temperature	hardness	250 °C 1 h/RT
400 °C, 100 h	400, 300, 200, and 100 °C	hardness	400 °C 100 h/400–100 °C
-	250 °C	Tensile	250 °C

3.1. Hardness Test at Room and high Temperature

Hardness test was carried out at room temperature after consolidation process (condition RT Table 2). Additionally, the effect of temperature on this property was also evaluated. In this regard, hardness was measured in two different conditions: at room temperature after compacts were heat treated at 250 °C for 1 h (condition 250 °C 1 h/RT, Table 2), and at room temperature after compacts were subjected to a heat treatment at 400 °C for 100 h (condition 400 °C 100 h/RT, Table 2, respectively).

Figure 1 shows the hardness values at room temperature after samples were tested under conditions RT, 400 °C 100 h/RT and 250 °C 1 h/RT. Regarding the first condition (RT), a high increase is observed in the hardness values of compacts prepared from vacuum milled aluminium (V), compared to those prepared from as-received aluminium (AR Al). This behaviour is mainly due to strain hardening produced by the intense plastic deformation of the Al particles during the milling process (30 hV for AR Al versus 102 hV for V compacts) [20]. An additional increase takes place as a result of ammonia gas incorporation to the milling process (102 hV for V versus 166 hV for F5 compacts). Furthermore, an improvement of this property can be observed as ammonia gas milling time is prolonged (F5 versus F10 and C), obtaining an increase in hardness of up to 18 hV. In this way, higher hardness values than those of the commercial alloys EN AW 2024 T4 and EN AW 7075 T6 (137 and 175 hV, respectively) are attained.

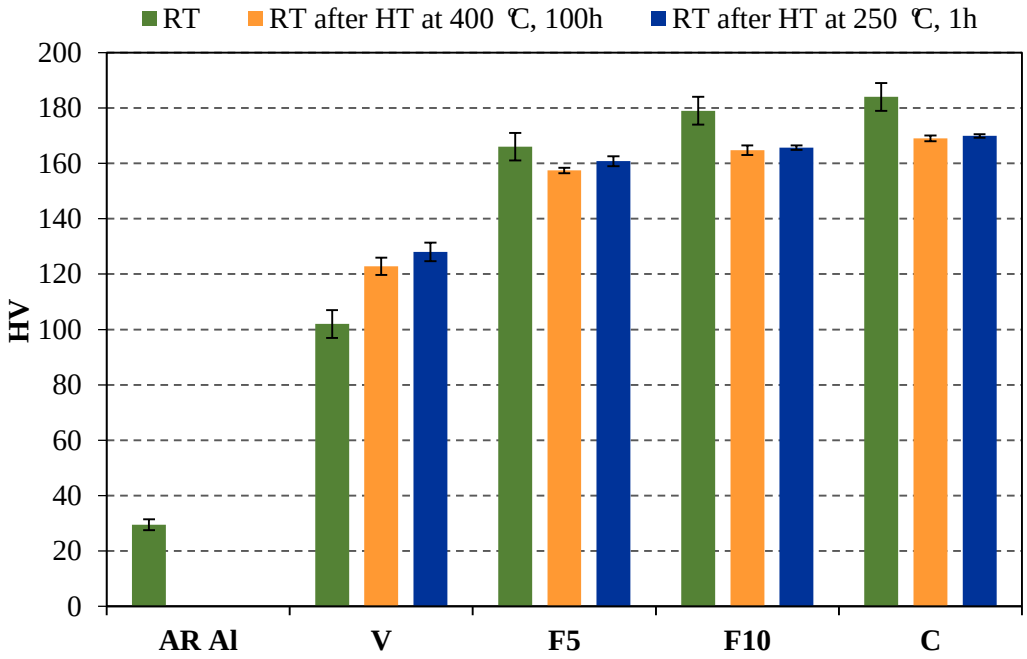

Figure 1. Vickers hardness measured at room temperature with (RT after hT at 400 °C, 100 h and RT after hT at 250 °C, 1 h) and without (RT) a previous heat treatment.

Accordingly, hardening effect is caused by two facts: strain hardening because of the energy transferred to the powders during mechanical alloying process, and the nitrogen incorporation into the aluminium lattice during milling. This nitrogen, in solid solution, forms refractory dispersed phases that significantly harden the material [21,22]. In order to evaluate the solid–gas reactions in the formation of new phases as a result of the milling process and the effect of temperature during heat treatments, XRD analysis were performed (Figure 2). Specifically, XRD were studied after both the sintering process and the most severe heat treating, 400 °C for 100 h (Figure 2a,b, respectively). In both cases, in addition to the Al peaks, reflections corresponding to aluminium carbide (Al_4C_3) and aluminium oxide (Al_2O_3) are detected in all samples. On the other hand, if ammonia gas is used during millings (F5, F10, and C), reflections corresponding to nitrogen-rich second phases (Al_4CON and Al_5O_6N) also appear. It is known that carbides arise from the EBS used as the PCA, the oxides come from the surface of the aluminium particles, and nitrides formation is due to ammonia gas dissociation during the mechanical alloying process. The XRD patterns were also fitted via Rietveld refinement [23] to quantify the phases formed. Data used for the refinement comes from the International Center for Diffraction Data (ICDD) PDF4 database [24]. Tables 3 and 4 collect the weight percentage of each phase in the different sintered and heat-treated compacts, respectively.

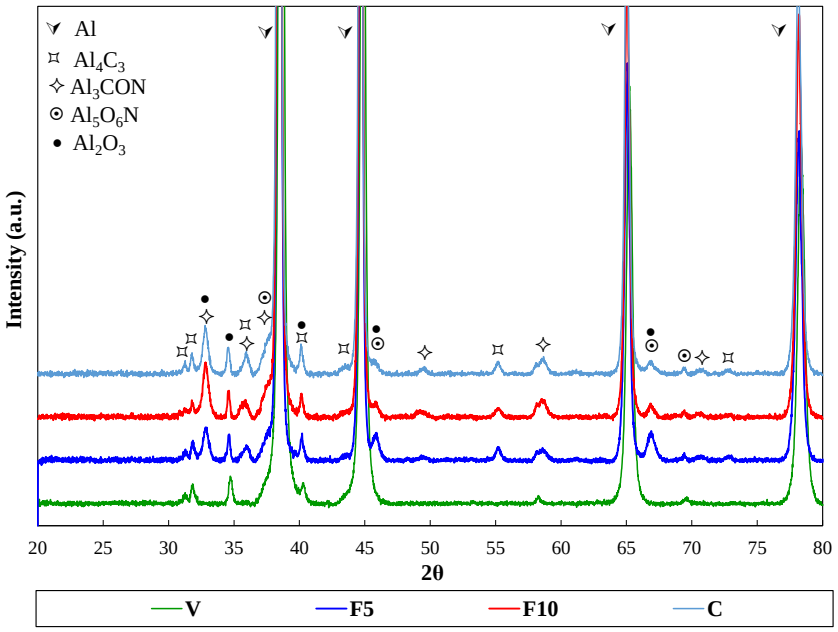

(**a**)

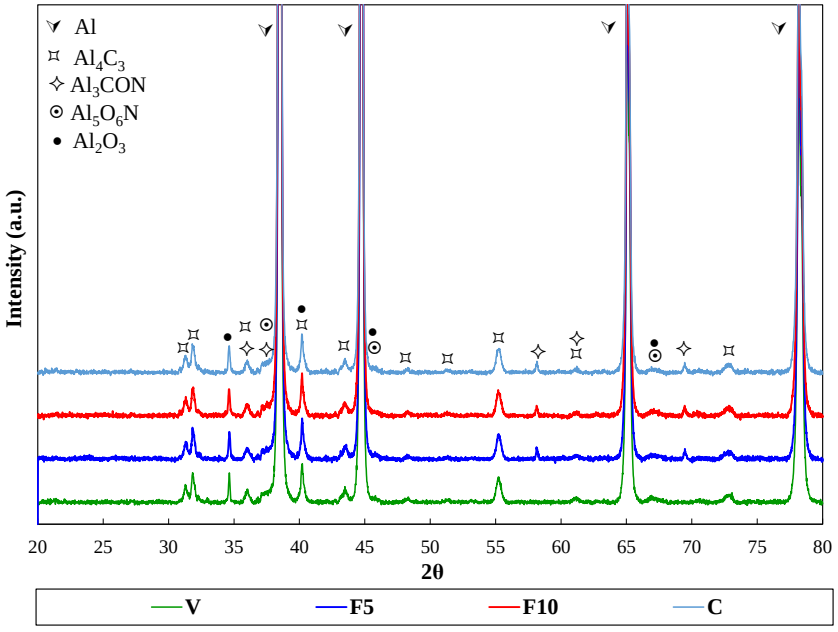

(**b**)

Figure 2. XRD patterns of the different samples after being (**a**) sintered and (**b**) heat treated at 400 °C for 100 h.

Table 3. Weight percentage of the phases in the different sintered samples.

Sample	Phase (Weight Percentage)					Fitting Parameter *Rwp*
	Al	Al_4C_3	Al_3CON	Al_5O_6N	Al_2O_3	
V	90	8	-	-	2	5.61
F5	86	4	4	3	3	6.32
F10	86	2	6	3	3	7.03
C	85	3	6	3	3	5.17

Table 4. Weight percentage of the phases after applied a heat treatment (400 °C, 100 h).

Sample	Phase (Weight Percentage)					Fitting Parameter *Rwp*
	Al	Al_4C_3	Al_3CON	Al_5O_6N	Al_2O_3	
V	93	5	-	-	2	5.43
F5	90	4	2	2	2	6.47
F10	90	4	2	2	2	6.92
C	90	4	2	2	2	5.33

After sintering, a slight growth in the weight percentage of aluminium oxycarbonitride (Al_4CON) from 4% up to 6% (samples F5 versus F10 and C, respectively) can be seen with the amount of time that ammonia gas was incorporated to the milling vessel (Table 3). In contrast, the weight percentage of aluminum oxynitride (Al_5O_6N) is kept at 3% for all samples milled in the presence of ammonia gas (F5, F10, and C).

On the other hand, hardness was measured in all the compacts after having been heat treated under conditions 400 °C 100 h/RT and 250 °C 1 h/RT listed in Table 2. Comparing the hardness values measured at room temperature (Figure 1), it can be observed that in general, hardness decreases as a result of the additional heat treatment applied (conditions 400 °C 100 h/RT and 250 °C 1 h/RT, Table 2). It should be highlighted that hardness values are similar in both 400 °C 100 h/RT and 250 °C 1 h/RT cases, despite the great differences in temperature and time in both heat treatments. In this way, it seems that hardness decreases because of temperature (250 °C, 1 h), but it does not decrease much more with increasing temperature and exposure time (400 °C, 100 h). It should be pointed out that even after being heated for a long time (condition 400 °C 100 h/RT), the hardness of the samples F5, F10, and C is still higher than that of the widely used commercial alloys (137 hV for EN AW 2024 T4 and 175 hV for EN AW 7075 T6). This result is even more remarkable considering that these commercial alloys were not subjected to any prolonged heat treatment.

XRD analysis show that once the compacts are heat treated, the amount of second phases (Table 4) is reduced with respect to the ones obtained after the sintering process. It seems that the prolonged heat undergone by the samples tends to decompose the second phases formed during the sintering process. Thus, the weight percentage of second phases decreases as that of the aluminium increases. Nevertheless, it is noteworthy that the decomposition of such second phases is very slow, if it is taken under consideration that the heat treatment at 400 °C lasted 100 h. In fact, after the heat treatment, more than half of the original amount of second phases is kept (around 15 wt % after sintering process versus 10 wt % after heat treatment). In addition, despite this prolonged annealing, samples F5, F10, and C achieved hardness values (157, 165, and 169 hV, respectively) higher than those of the commercial alloy EN AW 2024 T4 (137 hV) in the absence of such annealing.

Finally, a study of the evolution of hardness with temperature after a high temperature long-term annealing was carried out. Compacts were heated at 400 °C for 100 h and, after that, the temperature was decreased and hardness was measured at different temperatures ranging from 400 °C to room temperature (condition 400 °C 100 h/400–100 °C in Table 2). In this way, hardness versus temperature evolution is plotted in Figure 3. As might be expected, the hardness decreases with increasing temperature for all samples. Nevertheless, it must be highlighted that a remarkable improvement

is achieved because of the ammonia gas incorporation to the milling process. As can be seen, the hardness corresponding to F5 compacts undergoes an important improvement respect to V compact. Additionally, hardness increases are observed as the exposure time under ammonia gas is prolonged (compacts F10 and C). It is worth noting the notably improvement that the ammonia gas provokes in hardness, even at different temperatures. In particular, at 300 °C, hardness remains above 100 hV for F5, F10, and C specimens, while at room temperature, the highest hardness achieved for V compacts is only 90 HV.

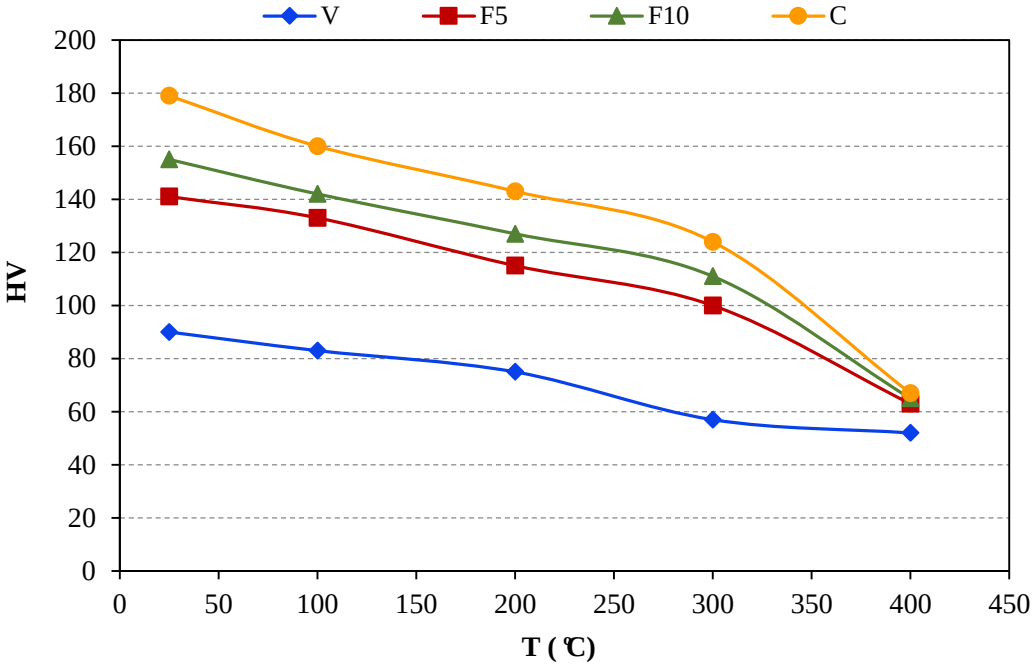

Figure 3. Vickers hardness at high temperature.

3.2. Tensile Test at Room and high Temperature

The effect of temperature on tensile properties was also evaluated using two different ways. Firstly, tensile test was carried out at room temperature, both after the consolidation process (condition RT, Table 2) and after compacts were previously heat treated at 400 °C for 100 h (condition 400 °C 100 h/RT, Table 2). Secondly, the tensile specimens were also tested at 250 °C (condition 250 °C, Table 2).

Figure 4 collects the UTS values obtained for the different compacts under the aforementioned conditions. For condition RT, it can be observed that UTS increases in compacts made from powder milled in vacuum (V) with respect to the ones made from as-received Al powder (AR Al), due to strain hardening that takes place as a result of the intense and repeated deformation of Al particles during the milling process [20]. In this way, an increase in UTS values higher than 250% is achieved in V compacts (247 MPa) with respect to AR Al compacts (67 MPa). In addition, it can be observed that UTS values follow an increasing trend as the ammonia gas is prolonged during the milling process. Thus, UTS values at RT increase up to 75% and 548% in C compacts compared to V and AR Al compacts, respectively. In this case, the improvement achieved is due to the formation of nitrogen-rich second phases after the sintering process.

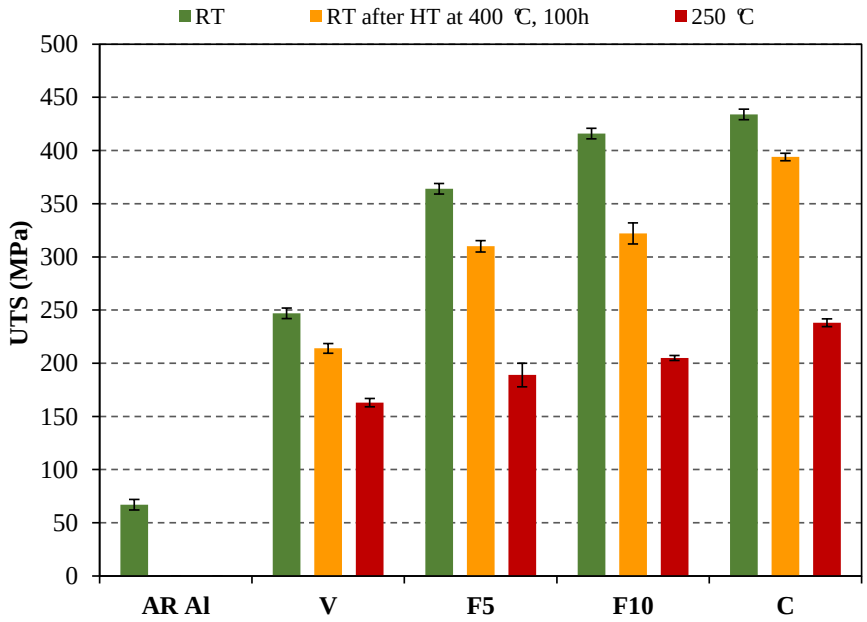

Figure 4. Ultimate tensile strength at room temperature with and without a previous heat treatment (400 °C, 100 h) as well as at high temperature (250 °C).

As expected, the UTS corresponding to conditions 400 °C 100 h/RT and 250 °C decreases as a consequence of temperature with respect to unheated specimens. Thus, tensile tests at 250 °C (condition 250 °C) provided lower UTS values than those of the one carried out at room temperature after specimens were heat treated at 400 °C for 100 h (condition 400 °C 100 h/RT). It is remarkable that compacts made from milled powder and tensile tested both under condition 400 °C 100 h/RT and 250 °C allow achieving UTS values much higher than those of the AR Al compacts. It must be highlighted that the UTS values observed at 250 °C remain above 163 MPa, which is significantly higher than those of commercial alloys EN AW 2024 T4 and EN AW 7075 T6, which reach UTS values lower than 100 MPa at 250 °C [25].

3.3. Fracture Surface Analysis

After the tensile test, the fracture surfaces were analysed. Macroscopically, compacts exhibit a flat fracture surface corresponding to a brittle failure. Figure 5 shows a tensile specimen made from powder milled under confined ammonia (C) and tensile tested at 250 °C. As can be seen, no signal of plastic deformation can be observed.

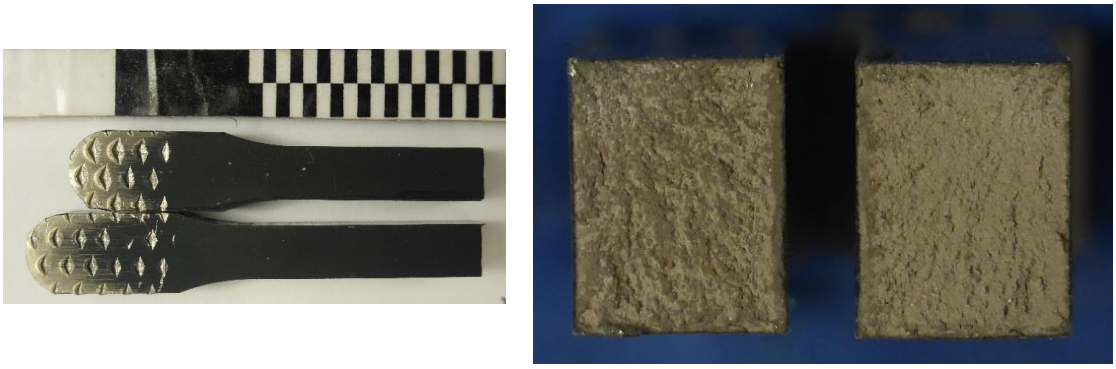

(**a**) (**b**)

Figure 5. (**a**) Longitudinal and (**b**) cross-section of tensile specimen C tested at 250 °C.

On the other hand, scanning electron micrographs, Figures 6 and 7, illustrate the fracture surfaces microscopically. All the specimens exhibit a surface consisting of a plentiful presence of dimples. The size of these dimples gets larger as the duration of the ammonia atmosphere is prolonged (F5, F10, and C). Dimples are formed as a result of the presence of hard particles in the ductile aluminium matrix. Accordingly, the probability of dimple formation also increases, making the already formed dimples easier to grow and coalesce [26]. In addition, a tensile test at 250 °C induces the softening of the aluminum matrix, which also contributes to increasing the size of the dimples. In this way, Figure 7d show a fracture surface where some small dimples with particles inside can be seen, and some larger dimples are also visible due to the growth and coalescence of voids during the tensile test at 250 °C. This morphology involves a certain level of plastic deformation at the microscopic level. however, the low ductility, as well as by the proportion of shallow dimples, is evidenced by the fact that an elongation lower than 1% is achieved for all samples.

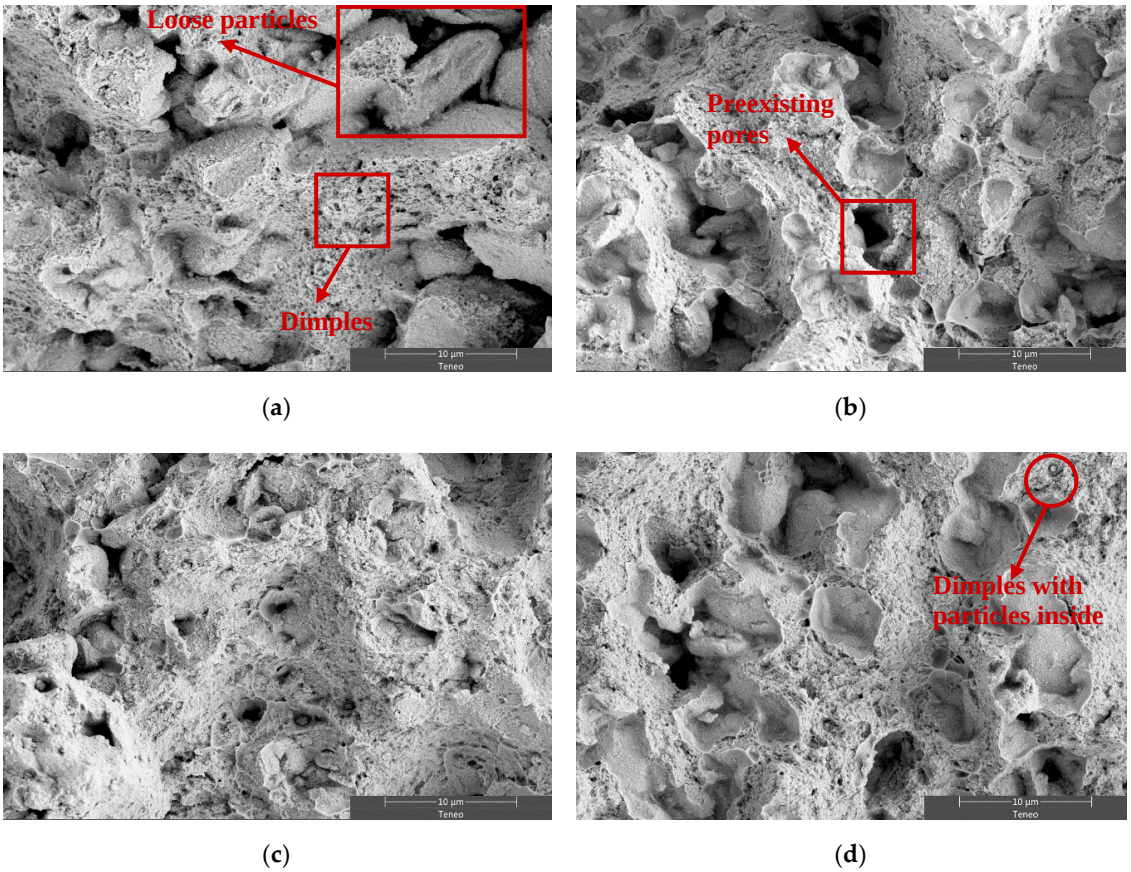

Figure 6. SE-SEM microfractographs of (**a**) V, (**b**) F5, (**c**) F10, and (**d**) C. A tensile test was carried out at room temperature after a heat treatment at 400 °C for 100 h.

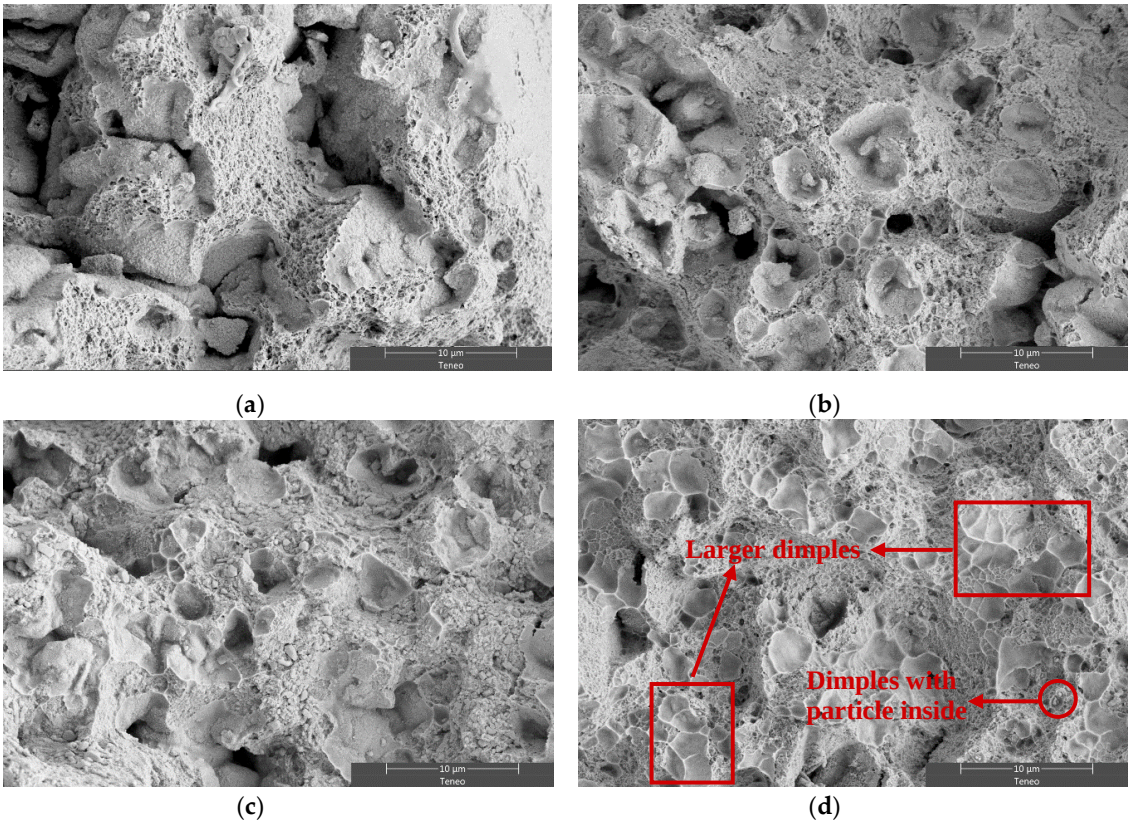

Figure 7. SE-SEM microfractographs of (**a**) V, (**b**) F5, (**c**) F10, and (**d**) C. A tensile test was carried out at 250 °C.

4. Conclusions

Aluminium powder was attrition-milled under three different atmosphere conditions (vacuum, confined ammonia gas, and a combination of vacuum and ammonia gas flow) and was consolidated by cold uniaxial pressing and vacuum sintering. After the consolidation process (condition RT), the results show that both hardness and UTS values increase due to the joint action of two mechanisms: the strain hardening of Al particles during the milling process and the formation of nitrogen-rich second phases after the sintering process, coming from the ammonia gas incorporated into the milling (F5, F10, and C). Subsequently, the degradation of their mechanical properties with temperature were evaluated. Results show that once compacts were submitted to a heat treatment (conditions 250 °C 1 h/RT and 400 °C 100 h/400–100 °C for hardness and 400 °C 100 h/RT and 250 °C for UTS), a slightly decrease is observed. XRD analysis showed that the prolonged heat undergone by the samples tends to decompose the second phases formed during the sintering process. Despite this, the hardness of the samples F5, F10, and C after being heated for a long time (condition 400 °C 100 h/RT) is still higher than that of the commercial alloy EN AW 2024 T4 (137 hV) and kept higher than 100 hV for a temperature of 300 °C. Regarding the UTS, compacts made from milled powder achieved values higher than those of the AR Al compacts and remained above 150 MPa at 250 °C. Furthermore, these values are significantly higher than those of commercial alloys EN AW 2024 T4 and EN AW 7075 T6, which reach UTS values lower than 100 MPa at 250 °C. This is due to the decomposition of the second phases being very slow despite the heat treatment at 400 °C lasting 100 h. In fact, XRD results showed that after such heat treatment, more than half of the original amount of second-phases is kept (around 15 wt % after the sintering process versus 10 wt % after heat treatment).

Author Contributions: Conceptualization, J.C. and F.G.C.; methodology, E.S.C. and F.G.C.; validation, F.T. and P.U.; formal analysis, E.S.C. and J.C.; writing—original draft preparation, E.S.C.; writing—review and editing, E.S.C., J.C. and F.G.C. All authors have read and agreed to the published version of the manuscript.

Funding: This research was founded by Ministerio de Economía y Competitividad (Spain) and FEDER (EU) through the research project DPI2015-69550-C2-1-P.

Acknowledgments: The authors also wish to thank the technicians J. Pinto, M. Madrid and M. Sanchez (University of Seville, Spain) for experimental assistance. We also thank the Microscopy and XRD Central Services (CITIUS, University of Seville).

Conflicts of Interest: The authors declare no conflict of interest.

References

1. Liu, J. Research development and application prospects of new aluminum alloy extruded-materials. *Mater. China* **2013**, *32*, 269–275.
2. Li, L.; Zhou, J.; Zhang, H. Advanced extrusion technology and application of aluminium, magnesium alloy for vehicle body. *J. Mech. Eng.* **2012**, *48*, 35–43. [CrossRef]
3. Sivananth, V.; Vijayarangan, S.; Rajamanickam, N. Evaluation of fatigue and impact behavior of titanium carbide reinforced metal matrix composites. *Mater. Sci. Eng. A Struct.* **2014**, *597*, 304–313. [CrossRef]
4. Huo, S.; Mais, B.; Gradl, J. Processing characteristics of alumix PM aluminum alloys. *Adv. PM Part Powder Met.* **2012**, *2012*, 7143–7154.
5. Hirsch, J.; Skrotzki, B.; Gottstein, G. *Aluminium Alloys: The Physical and Mechanical Properties*; John Wiley & Sons: hoboken, NJ, USA, 2008; Volume 1.
6. Lashgari, H.R.; Sufizadeh, A.R.; Emamy, M. The effect of strontium on the microstructure and wear properties of A356-10%B_4C cast composites. *Mater. Des.* **2010**, *31*, 2187–2195. [CrossRef]
7. Cintas, J.; Cuevas, F.G.; Montes, J.M.; herrera, E.J. Microstructural control of sintered mechanically alloyed Al-1%Ni material. *Scr. Mater.* **2005**, *52*, 341–345. [CrossRef]
8. Surappa, M.K. Aluminium matrix composites: Challenges and opportunities. *Sadhana Acad. Proc. Eng. Sci.* **2003**, *28*, 319–334. [CrossRef]
9. Tan, M.J.; Chew, M.C.; hung, N.P.; Sano, T.J. Thermal cycling processes in metal-matrix composites. *Mater. Process. Technol.* **1997**, *67*, 62–66. [CrossRef]
10. Cayron, C. Available online: http://cimewww.epfl.ch/people/cayron/Fichiers/thesebook-chap1.pdf (accessed on 23 July 2013).
11. Perng, C.C.; hwang, J.R.; Doong, J.L. Elevated-temperature, low-cycle fatigue behaviour of an Al_2O_{3p} 6061-T6 aluminium matrix composite. *J. Compos. Sci. Technol.* **1993**, *49*, 225–236. [CrossRef]
12. Fei, W.D.; hu, M.; Yao, C.K. Thermal expansion and thermal mismatch stress relaxation behaviors of SiC whisker reinforced aluminum composite. *Mater. Chem. Phys.* **2002**, *77*, 882–888. [CrossRef]
13. Chen, Y.C.; Daehn, G.S.; Wagoner, R.H. The potential for forming metal matrix composite components via thermal cycling. *Scr. Met. Mater.* **1990**, *24*, 2157–2162. [CrossRef]
14. Tjong, S.C.; Tam, K.F.; Wu, S.Q. Thermal cycling characteristics of in-situ Al-based composites prepared by reactive hot pressing. *Compos. Sci. Technol.* **2003**, *63*, 89–97. [CrossRef]
15. Sayman, O.; Ozer, M.R. Elastic-plastic thermal stress analysis of aluminum-matrix composite beams under a parabolically temperature distribution. *Compos. Sci. Technol.* **2001**, *61*, 2129–2137. [CrossRef]
16. Mizuuchi, K.; Inoue, K.; Agari, Y.; Morisada, Y.; Sugioka, M.; Tanaka, M.; Takeuchi, T.; Kawahara, M.; Makino, Y. Thermal conductivity of diamond particle dispersed aluminum matrix composites fabricated in solid-liquid co-existent state by SPS. *Compos. Part B* **2011**, *42*, 1029–1032. [CrossRef]
17. Sharma, S.; Nanda, T.; Pandey, O.P. Effect of elevated temperatures and applied pressure on the tribological properties of LM30/sillimanite aluminium alloy composites. *J. Compos. Mater.* **2019**, *53*, 1521–1539. [CrossRef]
18. Gao, Y.Y.; Dong, B.X.; Qui, F.; Wang, L.; Zhao, Q.L.; Jiang, Q.C. The superior elevated-temperature mechanical properties of Al-Cu-Mg-Si composites reinforced with in situ hybrid-sized TiCx-TiB2 particle. *Mater. Sci. Eng. A* **2018**, *728*, 157–164. [CrossRef]
19. Cintas, J.; Montes, J.M.; Cuevas, F.G.; Gallardo, J.M. Influence of PCA content on mechanical properties of sintered MA aluminium. *Mater. Sci. Forum* **2006**, *514–516*, 1279–1283. [CrossRef]
20. Caballero, E.S.; Cintas, J.; Cuevas, F.G.; Montes, J.M.; Ternero, F. Influence of milling atmosphere on the controlled formation of ultrafine dispersoids in Al-Based MMCs. *Metals* **2016**, *6*, 224. [CrossRef]
21. Caballero, E.S.; Cintas, J.; Cuevas, F.G.; Montes, J.M. Synthesis and characterization of in situ-reinforced Al–AlN composites produced by mechanical alloying. *J. Alloy. Compd.* **2017**, *728*, 640–644. [CrossRef]

22. Cintas, J.; Montes, J.M.; Cuevas, F.G.; herrera, E.J. heat-resistant bulk nanostructured P/M aluminium. *J. Alloy. Compd.* **2008**, *458*, 282–285. [CrossRef]
23. Young, R.A. *The Rietveld Method*, 1st ed.; Oxford University Press: New York, NY, USA, 1995.
24. *PDF4+ Commercial Database of the International Center for Diffraction Data*; ICDD: Newtown Square, PA, USA, 2019.
25. *Specific Metals and Alloys: Properties of Wrought Aluminium and Aluminium Alloys*; ASM handbook; ASM International: Materials Park, OH, USA, 1990; Volume 2.
26. Wang, F.; Li, J.; Xu, J.; Li, X.; Zhang, Y.; Wang, H. Investigation on fracture toughness of aluminum matrix composites reinforced with in situ titanium diboride particles. *J. Compos. Mater.* **2012**, *46*, 2145–2150. [CrossRef]